Larisa V. Fedorova, Vanamala Raju, Nasser El-Okdi, Amjad Shidyak, David J. Kennedy, Sandeep Vetteth, David R. Giovannucci, Alexei Y. Bagrov, Olga V. Fedorova, Joseph I. Shapiro and Deepak Malhotra

You might find this additional information useful...

This article cites 94 articles, 45 of which you can access free at:
http://ajprenal.physiology.org/cgi/content/full/296/4/F922#BIBL

Updated information and services including high-resolution figures, can be found at:
http://ajprenal.physiology.org/cgi/content/full/296/4/F922

Additional material and information about *AJP - Renal Physiology* can be found at:
http://www.the-aps.org/publications/ajprenal

This information is current as of June 17, 2009 .

The cardiotonic steroid hormone marinobufagenin induces renal fibrosis: implication of epithelial-to-mesenchymal transition

Larisa V. Fedorova,[1] Vanamala Raju,[1] Nasser El-Okdi,[1] Amjad Shidyak,[1] David J. Kennedy,[1] Sandeep Vetteth,[1] David R. Giovannucci,[2] Alexei Y. Bagrov,[3] Olga V. Fedorova,[3] Joseph I. Shapiro,[1] and Deepak Malhotra[1]

[1]*Division of Nephrology, Department of Medicine,* [2]*Department of Neuroscience, University of Toledo, College of Medicine. Toledo, Ohio 43614; and* [3]*Laboratory of Cardiovascular Science, National Institute on Aging, Baltimore, Maryland 21224*

Fedorova LV, Raju V, El-Okdi N, Shidyak A, Kennedy DJ, Vetteth S, Giovannucci DR, Bagrov AY, Fedorova OV, Shapiro JI, Malhotra D. The cardiotonic steroid hormone marinobufagenin induces renal fibrosis: implication of epithelial-to-mesenchymal transition. *Am J Physiol Renal Physiol* 296: F922–F934, 2009. First published January 28, 2009; doi:10.1152/ajprenal.90605.2008.—We recently demonstrated that the cardiotonic steroid marinobufagenin (MBG) induced fibrosis in rat hearts through direct stimulation of collagen I secretion by cardiac fibroblasts. This stimulation was also responsible for the cardiac fibrosis seen in experimental renal failure. In this study, the effect of MBG on the development of renal fibrosis in rats was investigated. Four weeks of MBG infusion triggered mild periglomerular and peritubular fibrosis in the cortex and the appearance of fibrotic scars in the corticomedullary junction of the kidney. MBG also significantly increased the protein levels and nuclear localization of the transcription factor Snail in the tubular epithelia. It is known that activation of Snail is associated with epithelial-to-mesenchymal transition (EMT) during renal fibrosis. To examine whether MBG alone can trigger EMT, we used the porcine proximal tubular cell line LLC-PK1. MBG (100 nM) caused LLC-PK1 cells grown to confluence to acquire a fibroblast-like shape and have an invasive motility. The expressions of the mesenchymal proteins collagen I, fibronectin, and vimentin were increased twofold. However, the total level of E-cadherin remained unchanged. These alterations in LLC-PK1 cells in the presence of MBG were accompanied by elevated expression and nuclear translocation of Snail. During the time course of EMT, MBG did not have measurable inhibitory effects on the ion pumping activity of its natural ligand, Na^+-K^+-ATPase. Our data suggest that the MBG may be an important factor in inducing EMT and, through this mechanism, elevated levels of MBG in chronic renal failure may play a role in the progressive fibrosis.

cardiotonic steroid hormone; ouabain; Na^+-K^+-ATPase; transcription factor Snail

CARDIOTONIC STEROIDS (CTSs), also known as cardiac glycosides or digitalis-like compounds, have been used for centuries to treat congestive heart failure. CTSs such as digoxin and digitoxin are still an important component of the clinical treatment of cardiac diseases (26, 65). CTSs were discovered in digitalis plants and amphibian tissues (25, 75). Recently, CTSs were found in the body fluids of mammals (5, 23, 29, 73). Moreover, elevated levels of endogenous CTSs including marinobufagenin (MBG) have been associated with various pathological conditions: essential hypertension (4, 24, 73), preeclampsia (3, 45, 83), experimental diabetes (7), uremic cardiomyopathy (33), and cardiac failure (20, 48, 49, 66, 74). MBG, like other CTSs, binds to the extracellular domain of the α-subunit of Na^+-K^+-ATPase (16, 21), which, in addition to its well-known function of maintaining cellular electrochemical balance through pumping sodium and potassium ions, can act as a typical membrane receptor (14, 28, 35, 55, 56, 73, 74, 84, 85, 88).

Our laboratory has reported recently that MBG is essential in the pathogenesis of cardiac fibrosis, which accompanies experimental renal failure (33). We have also observed that MBG treatment alone may induce fibrosis in the rat heart (20). Organ fibrosis is characterized by excessive deposition of extracellular matrix, which eventually leads to organ failure by impairment of its functions. Activated fibroblasts are key mediators of fibrogenesis. Mounting evidence suggests that the development of renal fibrosis includes the activation of resident interstitial fibroblasts as well as expansion of the fibroblasts pool through epithelial-to-mesenchymal transition (EMT; Refs. 17, 18, 62, 69, 91). During the course of EMT, epithelial cells loose their phenotypic and biochemical characteristics and acquire typical features of mesenchymal cells (30, 57, 86). EMT is essential at certain stages of embryogenesis (gastrulation, neural crest formation, and somitogenesis), but in an aging organism under pathological conditions (e.g., injury or inflammation) EMT can potentially lead to fibrosis of normal tissue or metastatic invasion of epithelial tumor cells (11, 27, 78). During the course of EMT, epithelial cells progressively redistribute or downregulate their apical and basolateral epithelial specific tight and adherent junction proteins and reexpress mesenchymal proteins like vimentin, fibronectin, and collagen I. This transition to mesenchyme is accompanied by the loss of cell-cell contacts and the gain of cell motility (30, 32, 86). EMT in renal tubular cells can be triggered by different growth factors (78, 91) and by stimuli such as aldosterone (93), oxidative stress (71), hypoxia (47), mechanical stretch (72), cyclosporine A (52), oncostatin M (61, 67), and advanced glycation end products (40).

We hypothesized that MBG could promote renal fibrosis through EMT as well. First, because the elevated levels of MBG, or its analogs, accompany the conditions at which EMT occurs, including end stage renal disease (34), normal pregnancy, and preeclampsia (3, 45, 68, 83). Second, the interaction of MBG with the Na^+-K^+-ATPase activates Src and ERK1/2 protein kinase pathways and increases the production of reac-

tive oxygen species (20, 33, 35, 80, 81). Finally, as it was shown for ouabain, MBG possibly can trigger phosphoinositide 3-kinase/protein kinase B (Akt) axis, stimulate NF-κB, and elevate the concentration of intracellular Ca^{2+} concentration (44, 55, 84, 88). Activation of these signaling pathways has been found to promote EMT in various animal and cellular models (11, 70, 78).

To test this hypothesis, MBG was administered to rats through a minipump for 4 wk. At the same time, we treated the porcine renal proximal tubular cell line LLC-PK1 with different concentrations of MBG and ouabain for up to 96 h. Several different aspects of EMT were analyzed including accumulation of collagen I in the kidney, expression of epithelial/mesenchymal marker proteins, and transcription factors/regulators known to be involved in EMT, and also alterations in cell morphology and acquisition of invasive motility in LLC-PK1 cells.

MATERIALS AND METHODS

Chemicals of the highest purity available were obtained from Sigma (St. Louis, MO). Radioactive rubidium ($^{86}Rb^+$) was obtained from Dupont NEN Life Science Products (Boston, MA). MBG was isolated from toad venom (Bufo Marines) as described previously (6).

Animals and animal model. The animal studies were approved by the University of Toledo Health Science Campus Institutional Animal Use and Care Committee. Male, Sprague-Dawley rats were used for all of the studies. Rats weighting ~250 g were subjected either to sham surgery or to osmotic minipump placement. MBG (10 μg/kg) was infused for period of 4 wk as described previously (20, 33).

Renal morphology and immunohistochemistry. Kidneys for light microscopy and immunoperoxidase staining were fixed in formalin and embedded in paraffin. Kidney sections (4 μm) were stained with saturated picric acid containing 0.1% Sirius red (Sigma) for 1 h in the dark. For immunoperoxidase staining, deparaffinized and rehydrated renal sections were blocked with 10% goat serum and 3% BSA (both from Sigma) in PBS for 2 h at room temperature. Primary antibodies against Snail (Abcam, Cambridge, MA) were diluted 1:400 in 5% goat serum and 3% BSA and applied to renal sections overnight at 4°C. After being washed, the sections were treated as suggested by ABC protocol (ABC Elite kit; Vector Laboratories, Burlingame, CA) and counterstained with methyl green. Immunoperoxidase staining of kidney sections for α-smooth muscle actin (α-SMA) was preformed with α-SMA kit (Sigma) with NovaRed chromophore (Vector Laboratories) and counterstained with methyl green. Bright light and polarized images of picosirius red and α-SMA were taken on a Nikon Eclipse 80i microscope equipped with a Nikon camera head DS-Fi1 (Nikon, Tokyo, Japan) or Olympus B microscope (Olympus Optical, Hamburg, Germany) with Evolution MP color digital camera (Media Cybernetics, Bethesda, MD) for Snail. For quantitative morphometric analysis, eight randomly chosen cortical fields (at least 6 from each animal from experimental group) lacking major blood vessels were digitized and the collagen volume determined using the Imager J software (National Institutes of Health) as previously described (33).

Cell culture. The porcine kidney proximal tubule cell line LLC-PK1 was obtained from the American Tissue Culture Collection (Manassas, VA). Cells were grown either on plastic culture plates for protein extraction or on glass slides for immunochemistry. LLC-PK1 cells were grown in DMEM (Sigma) containing 10% FBS (Hyclone, Logan, UT) and 1% penicillin streptomycin for 1–2 days until they reached 90–100% confluence. Before treatment, cells were serum starved for 12–18 h with serum free medium and then treated with different concentrations of MBG or ouabain ranging from 0.1 to 100 nM for up to 96 h. In control cells, the vehicle DMSO (≤0.01%) was added. In some of the experiments, cells were also treated with 5

to 10 ng/ml of TGF-β_1 (for up to 96 h). Fresh MBG and TGF-β_1 (Sigma) were added daily for the entire duration of treatment.

Preparation of whole tissue/cell lysates. Frozen (−80°C) tissues were grinded in liquid nitrogen and placed immediately into ice-cold RIPA containing 50 mM Tris·HCl pH 7.5, 150 mM NaCl, 1% Nonidet P-40 substitute, 5% sodium deoxychlorate, 0.1% SDS, protease inhibitors (0.2 mM 2-aminoethylbenzenesulfonyl fluoride, 8 μM bestatin, 2.8 μM E-64, 3 μM pepstatin, 4 μM leupeptin, and 0.16 μM aprotinin; Protease Inhibitor Cocktail, Sigma), and 1 mM EDTA. Cells were washed twice with ice-cold PBS and proteins were immediately extracted in RIPA buffer. Protein concentration was estimated by Bio-Rad protein assay (Hercules, CA).

SDS-PAGE, Western blotting, and autoradiography. SDS-PAGE was carried out using standard protocols. Proteins were transferred onto PVDF membrane by semidry method (38) using trans-Blot SD semidry transfer cell (Bio-Rad). Membranes were blocked in 5% nonfat dry milk in Tris-buffered saline, containing 0.1% Tween-20. The following antibodies were used at concentrations recommended by the respective manufacturer: mouse anti-E-cadherin from BD Biosciences, clone 36; rabbit anti-occludin and anti-claudin I from Zymed Laboratories (South San Francisco, CA), rabbit anti-β-catenin from Sigma, rabbit anti-Snail from Abcam (Cambridge, MA), mouse anti-vimentin from Serotec (Oxford, UK), rabbit anti-fibronectin from Chemicon (Temecula, CA), and goat anti-actin clone I-19 from Santa Cruz Biotechnology (Santa Cruz, CA). For all Western blots, secondary antibodies from Santa Cruz Biotechnology were used.

Cell invasion assay. To asses the invasive property of the transformed cells, LLC-PK1 cells were grown on collagen gels (2.5 mg/ml, 2.5-mm thick). Gels were made from rat tail collagen Type I from BD Biosciences (Bedford, MA) in sixwell plates according to company protocol. After the gel was polymerized, the surface was washed once with sterile PBS and once with 10% DMEM medium and then the cell suspension was added. Cells were grown up to 90–100% confluence before they were serum starved and treated with 100 nM MBG for 72 and 96 h. After treatment, the collagen gels were separated from the wells and the cells on the collagen gels were washed twice with cold PBS and fixed in 4% formaldehyde for 30 min at room temperature. Gels were incubated with 0.1% Coomassie (R250) in 10% methanol and 10% acetic acid until sufficient staining was achieved. The gels were then destained with 50% methanol and 10% acetic acid with frequent washings. The gels were later mounted on glass slides using gelatin mount from Sigma. Differential interference contrast images of cells on the gel surface as well as the invading collagen were taken on IX71 inverted research microscope (Olympus) focused on different planes.

Immunocytochemistry. Cells were grown on eightwell Lab-Tek II chamber slides under the conditions described above. After a specified time of treatment, cells were washed twice in PBS pH 7.4 and fixed in ice cold methanol for 10 min at 4°C. Cell walls were permeabilized with 4 mM sodium deoxycholate in PBS for 10 min at room temperature and then washed in PBS containing 0.025% Triton for 5 min. Nonspecific binding of the antibodies was blocked by incubation in PBS containing 1.5% normal horse serum from Vector Laboratories for 30–60 min depending on the antibody used. Cells were then incubated at room temperature for 1 h with primary antibodies. For immunocytochemistry, the same antibodies as for Western blotting were used except for E-cadherin and β-catenin staining. Prediluted mouse anti-E-cadherin and anti-β-catenin antibodies from Cell Marque (Rocklin, CA) were used as a manufacturer's suggestion. Immunoperoxidase staining of E-cadherin was done using an ABC Elite kit from Vector Laboratories. For fluorescent immunostaining, fluorescein-conjugated goat anti-mouse IgG and Oregon Green 488 goat anti-rabbit IgG from Invitrogen (Eugene, AR) diluted 1:200 were applied for 30 min in the dark.

Confocal images were captured by a spectral confocal scanner (model TCS SP2; Leica, Mannheim, Germany) and microscope

(model DMIRE2, Leica) equipped with a ×63.0 oil immersion objective.

Analysis of collagen I synthesis. Analysis of collagen I synthesis was performed as described by Strutz et al. (76) with some modifications. Cells were grown to total confluence in 12-well plates in the presence of 50 µg/ml ascorbic acid and 50 µg/ml propionitrile (both from Sigma) and treated with 100 nM MBG for 72 and 96 h as described in *Cell culture.* Supernatants (100 µl) were collected, transferred to 96 well plates (Nunc), and incubated overnight at room temperature. Plates were dried the following day for 2 h and blocked in incubation buffer, containing 1.5% normal horse serum (Vector Laboratories) in PBS at 37°C for 10 min. Rabbit polyclonal antibody against collagen I was added at dilution 1:2,000 (Abcam, ab292) in incubation buffer and probed for 2 h room temperature. The plates were then washed five times with a washing solution containing PBS and 0.02% triton followed by incubation with secondary antibodies (biotinylated goat-anti-rabbit; Bio-Rad) diluted 1:8,000 in incubation buffer for 1 h. The plates were washed five times, 5 min each, with washing buffer and left overnight for binding of streptavidin-horse-radish perioxidase conjugate (BD Bioscience) diluted 1:4,000 in incubation buffer in a cold room on a shaking apparatus. Finally, the plates were washed three times in washing buffer and incubated with *o*-phenylenediamine. When sufficient color was developed, the absorbance was measured at 490 nm at Spectra Max 250 plate reader (Molecular Devices). Assays were run in triplicates and repeated three times. Standardization was obtained using rat tail collagen, type I (BD Bioscience). Working range for the detection was from 100 ng to 2,500 ng/ml.

Preparation of nuclear fractions. The preparations of nuclear fractions were done as described previously (43). LLC-PK1 cells were incubated for 15 min on ice in hypotonic buffer containing 10 mM Tris·HCl, pH 7.2, and protease inhibitors cocktail (Sigma) diluted as described for RIPA buffer. After homogenization, the cell extracts were diluted with equal volume of 0.5 M sucrose in hypotonic buffer and centrifuged at 800 *g* for 10 min at 4°C. The pellet was resuspended, homogenized, and centrifuged at 430,000 *g* for 2 h to pass through a 2-M sucrose cushion. The nuclear pellets were resuspended in RIPA buffer and applied for Western blot analysis.

3-(4,5-dimethylthiazol-2-yl)-2,5-Diphenyltetrazolium bromide and lactate dehydrogenase viability assays. LLC-PK1 cells were grown to confluence in 96-well plates in DMEM containing 10% FBS as described above. Cells were serum starved overnight before treatment with MBG or ouabain. The viability of the cells was evaluated every 24 h, as suggested by protocols for 3-(4,5-dimethylthiazol-2-yl)-2,5-diphenyltetrazolium bromide (MTT)-based and lactate dehydrogenase (LDH)-based toxicology assay kits (Sigma).

Measurement of Na$^+$-K$^+$-ATPase activity. Na$^+$-K$^+$-ATPase activity was assessed by ^{86}Rb$^+$ uptake assay as described previously (42, 43). LLC-PK1 cells were grown to confluence and treated with MBG or ouabain as described in *Cell culture.* Monensin (20 µM) was added

to the medium before initiation of the ^{86}Rb$^+$ uptake to assure that maximal capacity of active uptake was measured. The uptake was initiated by addition of radioactive ^{86}Rb$^+$ and stopped after 10 min by addition of 0.1 M ice-cold MgCl$_2$. Intracellular ^{86}Rb$^+$ was precipitated with TCA and radioactive signal counted. The ^{86}Rb$^+$ uptake was calibrated with TCA-precipitated protein content for each treatment.
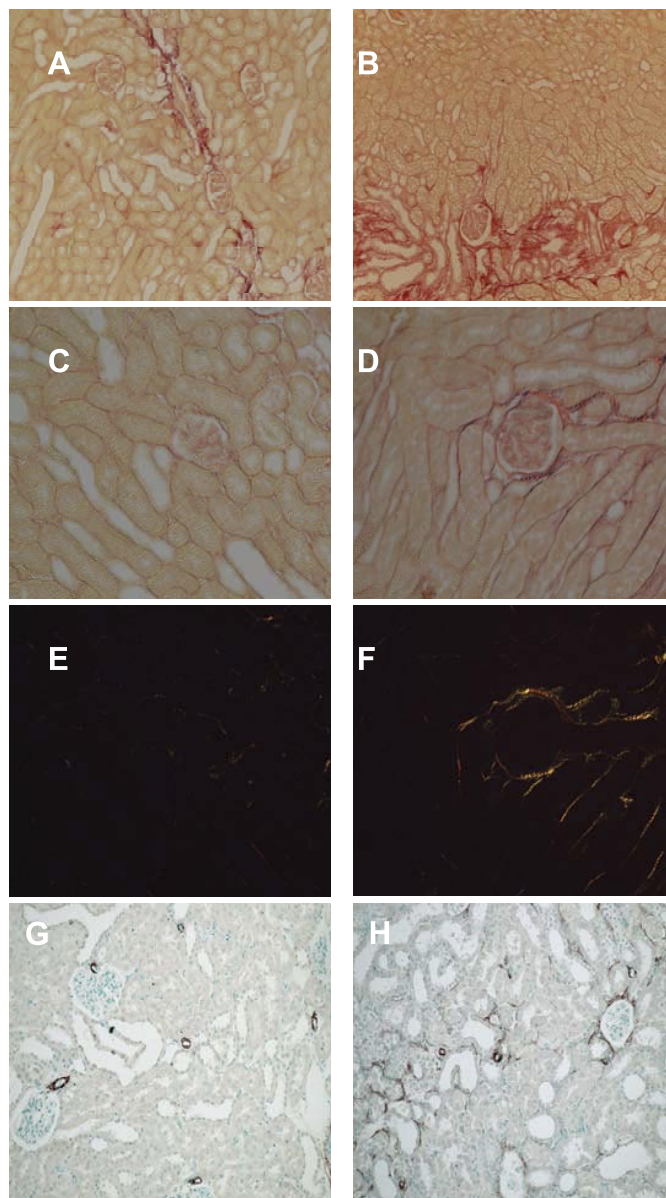

Fig. 1. Marinobufagenin (MBG) infusion to rats induced renal fibrosis. *A–H*: microphotograph images taken from control rats (*left*) and MBG-administrated rats (*right*). MBG administration induced significant accumulation of tubulointerstitial collagen proximal to interlobar and arcuate blood vessels (*A* and *B*). In the cortex, MBG administration resulted in development of peritubular and periglomerular fibrosis (*C–F*), as demonstrated by picosirius red staining imaged in bright (*C* and *D*) and polarized light (*E* and *F*). Development of periglomerular and peritubular fibrosis after MBG administration was confirmed by appearance of α-smooth muscle actin (α-SMA)-positive cells around renal corpuscle and in the tubulointerstitium (*G* and *H*). *I*: representative Western blot for proteins extracted from whole kidneys and probed against procollagen I antibodies. *J*: densitometry analysis of Western blots (*n* = 11 from more than 3 independent experiments; *P < 0.05 vs. control). *K*: results of computer-assisted morphometry measurements of collagen content in kidney intersitium (*n* = 20 from 3 independent experiments; *P < 0.05 vs. control).
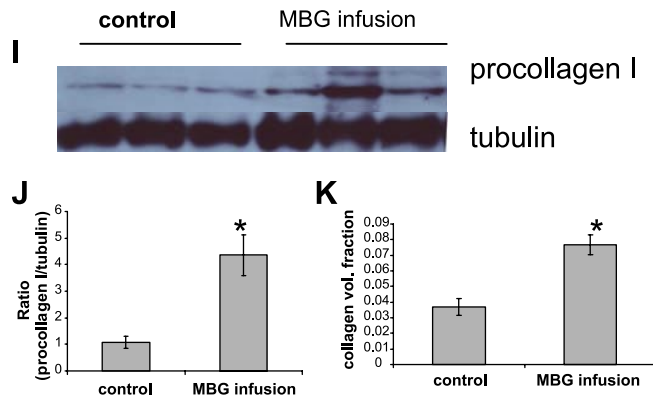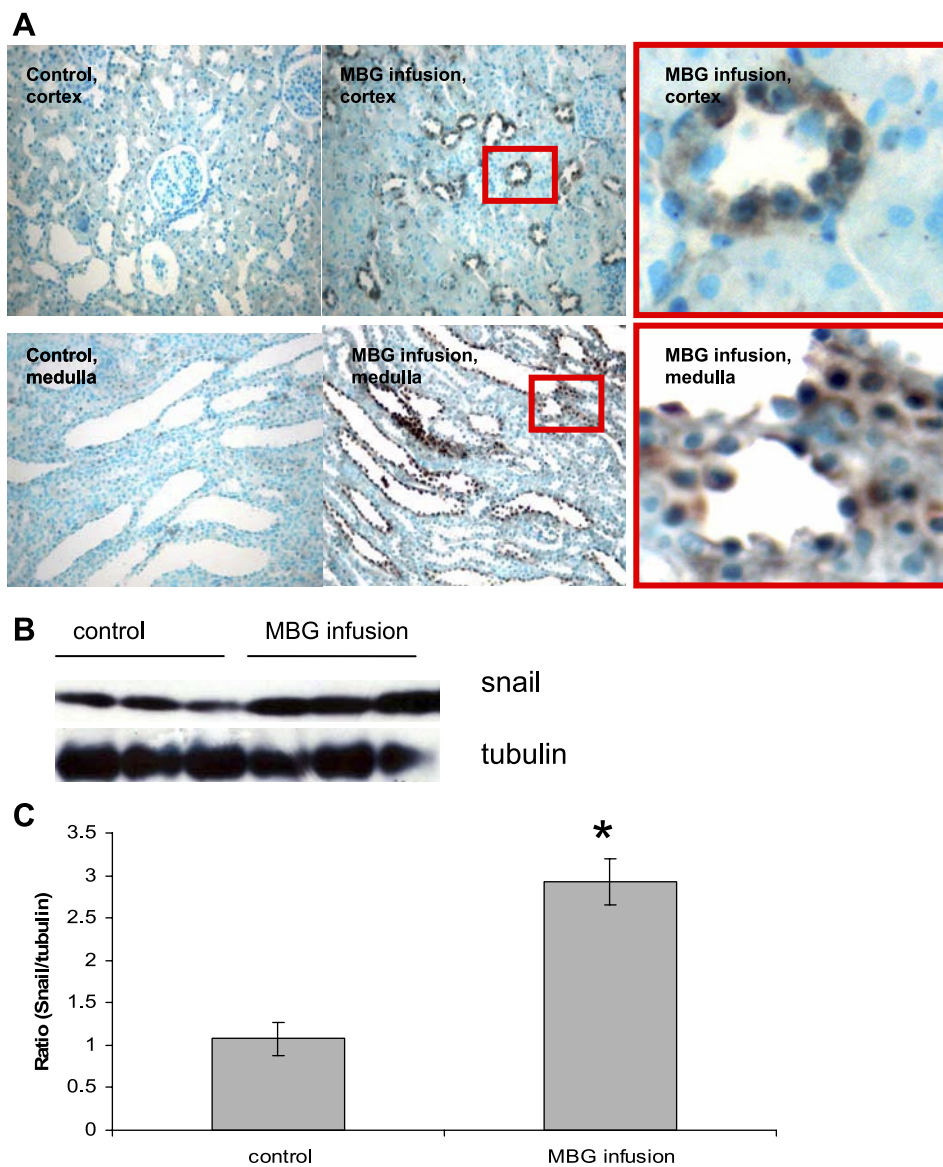
Fig. 2. MBG administration to rats induced upregulation and nuclear localization of the transcription factor Snail in tubular epithelia in cortex and in medulla (*A*). *B*: representative Western blot for proteins extracted from whole kidneys and probed against Snail protein. *C*: densitometry analysis of Western blots ($n = 15$ from more than 3 independent experiments; *$P < 0.05$ vs. control).

Statistical analysis. Data are presented as means ± SE. Unpaired Student's *t*-test was used to evaluate the difference between groups. Statistical significance was reported at the $P < 0.05$ and $P < 0.001$ levels.

RESULTS

MBG induces alterations of physiological parameters and renal fibrosis in rats. MBG infusion to rats for 4 wk resulted in an increase of plasma levels of MBG from 359 ± 16 to 546 ± 36 pmol/l, aldosterone from 191 ± 55 to 322 ± 38 pg/ml, and systolic blood pressure from 102 ± 2 to 136 ± 4 mmHg. Kidney sections of MBG-supplemented and control rats were stained with collagen specific picosirius red. Fibrotic lesions with significant accumulation of collagen I around tubules were found in the area proximal to the interlobar and the arcuate vessels (Fig. 1, *A* and *B*). Furthermore, MBG infusion induced periglomerular and peritubular accumulation of collagen I (although to a lesser extend) in renal cortex, as demonstrated in the photomicrographs of picosirius red stained kidney sections taken in bright and polarized light (Fig. 1, *C–F*).

Accumulation of interstitial collagen I fibers in the kidney cortex estimated by imaging of picosirius red stained sections revealed a twofold increase with MBG infusion (Fig. 1*K*). The development of periglomerular and peritubular fibrosis in MBG-treated rats was further supported by the presence of the α-SMA-positive cells around the renal corpuscles and in the tubular interstitium (Fig. 1, *G* and *H*). Western blotting of whole kidney extracts showed that procollagen I expression was increased four times in rats supplemented with MBG (Fig. 1, *I* and *J*). Therefore, 4 wk of MBG infusion induced activation of matrix-producing perivascular and periglomerular mesenchymal cells and consequent secretion of collagen I fibers in the renal cortex, the corticomedullary junction, and the columns of Bertini. This effect of MBG could be due to renin-angiotensin-aldosterone system induced TGF-β_1 upregulation. Indeed Western blotting of whole kidney extracts showed upregulation of TGF-β_1 after MBG treatment (data not shown).

In contrast to mainly perivascular and periglomerular activation of mesenchymal cells, the profibrotic transcription fac-
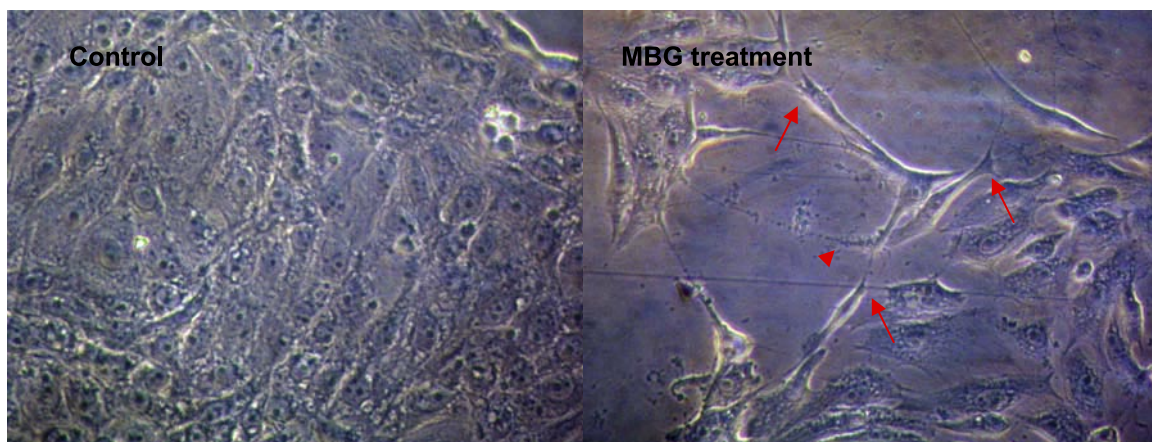
Fig. 3. Phase contrast images of LLC-PK1 cells grown for 96 h on poly-D-lysine coated slides. In the presence of 100 nM of MBG, epithelial cells acquired mesenchymal features, spindle-like shape, filopodias on the moving edge (arrows) and trailing tail (arrowhead).

tor Snail, a key regulator of EMT, was found de novo expressed in both cortical and medullary tubular epithelial cells in MBG-treated kidneys (Fig. 2). Moreover, in some epithelial cells the Snail protein was specifically located inside the nuclei. Western blotting of proteins extracted from whole kidneys showed a threefold increase of Snail protein expression after MBG infusion. The basal level of Snail present in the extracts from control kidneys reflects the expression of Snail protein in the muscularis layer of the renal calyx (not shown). Surprisingly, Western blotting of proteins from whole kidney tissues as well as immunohistochemical analysis of kidney sections did not reveal any changes in the expression and cellular localization of the epithelial markers E-cadherin and β-catenin with MBG administration (not shown).

Effect of MBG on LLC-PK1 cells morphology. The proximal tubular epithelial cell line LLC-PK1 was chosen for our in vitro studies because these cells have been intensively used in our laboratory for investigation of the mechanism of ouabain signaling through the Na^+-K^+-ATPase signalosome. We treated subconfluent (~50%) and confluent cultures of LLC-PK1 cells with MBG or ouabain in concentrations of 0.1, 1.0, 10.0, 50, and 100 nM, and TGF-β_1 (5–10 ng/ml) as a positive control for EMT. The morphological changes of the cells were monitored at 24, 48, 72, and 96 h. Control LLC-PK1 cells formed a strong epithelial sheet characterized by cobblestone-like morphology typical for epithelial cells (Fig. 3). Clear changes in cellular morphology to fibroblast-like cells were observed only in confluent cultures treated with MBG for 72 and 96 h at 100 nM and to some extent at 50 nM (not shown). Ouabain, another CTS, did not induce alterations in the LLC-PK1 cells that were noted with MBG in all our experiments. Fibroblast-like cells were absent in confluent culture of LLC-PK1 cells treated with TGF-β_1 and in subconfluent cultures treated either with ouabain or MBG. It has been shown earlier by Masszi et al. (51) that the confluent cultures of LLC-PK1 cells are resistant to TGF-β_1-induced EMT and that only subconfluent cultures showed EMT-like alterations in the presence of TGF-β_1. The morphological features of the transformation of LLC-PK1 cells induced by 100 nM MBG for 96 h to cells resembling the mesenchymal phenotype occurred to a greater extent while the cells were at confluence rather than other experimental settings. Therefore, all further experiments

were performed only at conditions in which the LLC-PK1 cells had achieved confluent monolayers.

The viability of the LLC-PK1 cells was assessed after treatment with cardiotonic steroids at 24, 48, 72, and 96 h by MTT- and LDH-based toxicity assays. As determined by these two assays, there were no lethal effects on the LLC-PK1 cells by 100 nM MBG during the examined time points. The results of viability by the MTT assay for LLC-PK1 cells treated for 24 h are shown in Table 1. MBG even at a concentration of 250 nM did not have any toxic effect on LLC-PK1 cells at 24 h. At the same time, ouabain in concentrations 50 and 100 nM, at which MBG triggers EMT-like morphological alterations of LLC-PK1 cell, induced cell death by 15 and 25%, respectively, even after 24 h of treatment.

EMT is generally characterized by acquisition of morphological features specific for fibroblasts and increased cells migration and invasion. Epithelial cells in confluent monolayer are not motile at all. To test whether MBG induces invasive motility, we seeded cells on collagen I gel and analyzed invasion of the cells into the collagen matrix (Fig. 4, *A* and *B*). We found that after 72 h of MBG treatment while many cells still are incorporated in patches of epithelial sheet, ~30% of LLC-PK1 cells are scattered. After 96 h >20% are scattered on the surface of the gel and ~40% of the total number of cells

Table 1. *Effect of MBG and ouabain on viability of LLC-PK1 cells and pumping activity of Na^+-K^+-ATPase*

	MTT Staining, %	Maximal Na^+/K^+ Pump Activity
Control	100.0±3.8	100.0±4.8
100 nM MBG	106.7±2.3	91.8±7.8
250 nM MBG	105.5±3.7	76.3±5.6*
10 nM ouabain	106.0±3.1	NA
50 nM ouabain	86.6±3.9*	37.6±4.9†
100 nM ouabain	74.8±1.4†	30.0±0.6†

Viability of LLC-PK1 cells in the presence of ouabain and marinobufagenin (MBG) was estimated by 3-(4,5-dimethylthiazol-2-yl)-2,5-diphenyltetrazolium bromide (MTT) staining, and pumping activity of Na^+-K^+-ATPase was determined by $^{86}Rb^+$ uptake after 24-h treatment with cardiotonic steroids (CTSs). MTT staining and the pumping activity at the absence of CTSs were taken as 100%. Means ± SE from more than 3 experiments performed in sextuplicates are shown. *$P < 0.05$, †$P < 0.001$ vs. control.
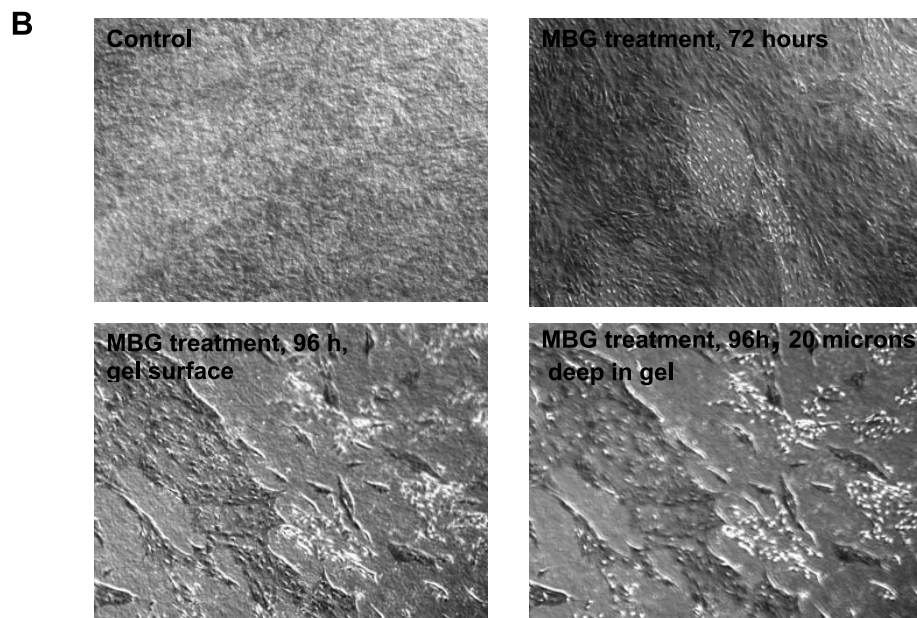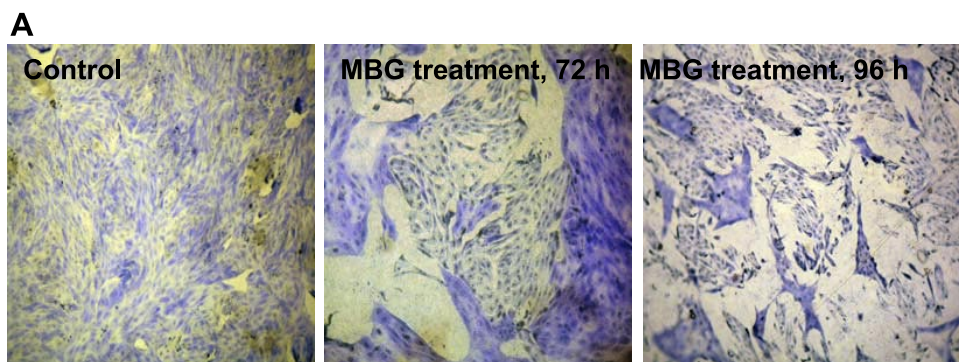
A

B

Fig. 4. LLC-PK1 cells grown on collagen I gel changed their morphology from epithelial to fibroblast-like and invaded collagen. *A*: LLC-PK1 cells grown on collagen I gel were stained with Coomassie. *B*: differential interference contrast images of LLC-PK1 cells grown on collagen gel. In control, untreated cultures of epithelial cells completely covered the surface of collagen gel. After 72 h of treatment with 100 nM MBG, ∼30% of cells were scattered and acquired mesenchymal phenotype, but the majority of these cells were still located on the surface of collagen gel. After treatment with 100 nM of MBG for 96 h, >60% of the LLC-PK1 cells acquired fibroblast-like shape and 40% of the cells invaded the collagen gel. *C*: at least 5 random fields of LLC-PK1 cells grown on each collagen gel ($n = 10$, for each time point) were captured and number of cells on the surface or in the gel were counted. $*P < 0.05$ vs. control.

C
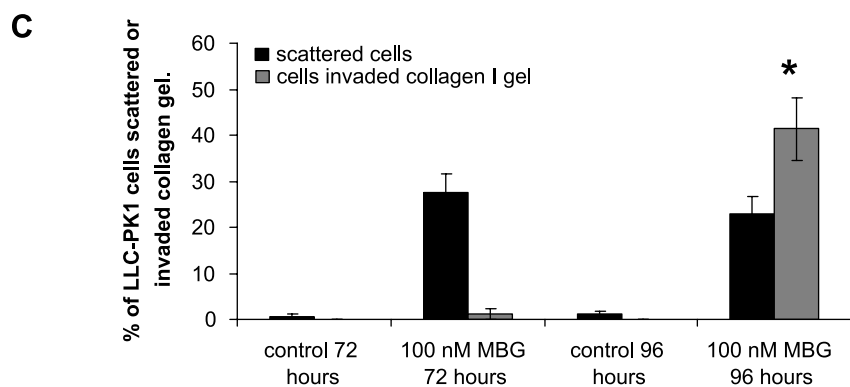
indeed invaded the collagen matrix (Fig. 4*C*). There were no cells found in the collagen matrices in control cultures or cultures treated with MBG for 72 h.

Effect of MBG on the expression of epithelial proteins. It has been shown previously that LLC-PK1 cells are resistant to TGF-β_1-induced EMT in intact confluent monolayer and are susceptible to EMT if formation of cell-cell contacts is prevented by different experimental conditions including low density (51). In this so-called contact-dependent model of TGF-β_1-induced EMT of LLC-PK1 cells, treatment with TGF-β_1 triggered dramatic downregulation of E-cadherin, a

major marker of epithelial phenotype after 72 h posttreatment. In our initial experiments when confluent and subconfluent cultures LLC-PK1 cells were treated with TGF-β_1, these findings were confirmed. When we treated subconfluent (50–60% of cell density) cultures of LLC-PK1 cells with MBG in concentration from 0.1 to 100 nM up to 96 h, we documented downregulation of E-cadherin protein level as well (data are not shown).

Immunocytochemical staining of the MBG-treated confluent monolayer of LLC-PK1 cells showed that fibroblast-like cells, which are completely detached, did not express E-cadherin on
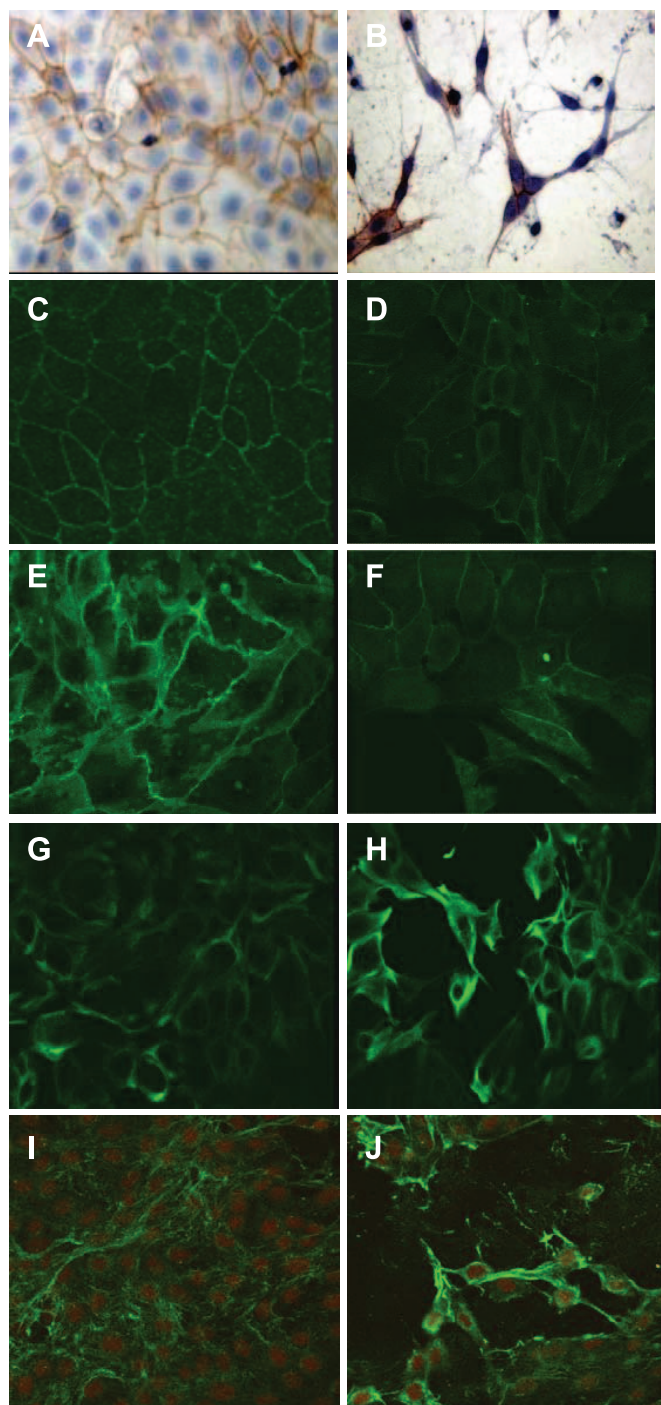
their surfaces (Fig. 5). At the same time, there were cells that demonstrated mesenchymal features as spindle-like shape and filopodias; however, these cells remained attached to the neighboring cells by their cellular membranes. These cells demonstrated intensive staining for E-cadherin at the sites of contacts. Western blotting analysis of cell lysates from MBG-treated cultures revealed that the total level of E-cadherin protein remained unchanged (Fig. 6). High levels of total E-cadherin protein expression in LLC-PK1 total cell extracts, despite massive detachment and scattering of cells induced by MBG treatment, can be explained by the long half-life of the E-cadherin protein. A similar discrepancy has been demonstrated in other cell systems (64, 76). The half-life of E-cadherin is estimated to be >40 h (46). Overall, these data suggest that in an MBG-induced model of EMT in LLC-PK1 cells, unlike a majority of EMT models, downregulation of E-cadherin does not preclude or induce EMT.

We investigated the effects of MBG treatment on expression of the core tight junction proteins occludin and claudin I. At 72 h of treatment, cells were detached from each other, yet they still expressed considerable amount of claudin I and occludin (Fig. 5) around the cellular membranes. However, after 96 h of treatment, the transformed cells were characterized by more dispersed specific staining for tight junction proteins. Western blots run with extracts from LLC-PK1 cells showed that MBG decreased expression of claudin I by 30% at 96 h posttreatment (Fig. 6), while the level of occludin remained unchanged (Fig. 6).

Effect of MBG on the expression of mesenchymal proteins. To further investigate whether MBG indeed promotes EMT in LLC-PK1 cells, we analyzed the expression of the mesenchymal marker proteins fibronectin, vimentin, and collagen I.

Fig. 5. Indirect immunofluorescence staining for epithelial marker proteins E-cadherin (*A* and *B*), occludin (*C* and *D*), claudin I (*E* and *F*), and mesenchymal marker proteins vimentin (*G* and *H*), and fibronectin (*I* and *J*). *Left*: shows immunostaining of control LLC-PK1 cells grown for 96 h; *right*: LLC-PK1 cells grown in the presence of 100 nM of MBG for 96 h. Completely detached cells with fibroblast like morphology do not show E-cadherin specific staining, while transformed cells still attached to each other express E-cadherin at their contact sites. MBG treatment induced marked redistribution of tight junction proteins occludin I and claudin and increased staining for mesenchymal markers vimentin and fibronectin.
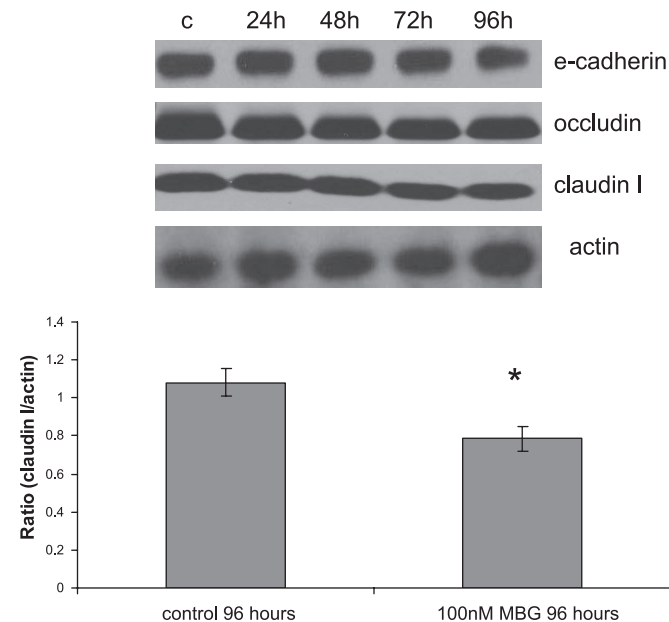

Fig. 6. MBG treatment did not induce any changes in the level of adherent junction protein E-cadherin, insignificantly reduced level of tight junction protein occludin, and decreased level of claudin I by 30%. Representative Western blot of proteins extracted from control and MBG-treated (100 nM) LLC-PK1 cells at 4 time points and probed with antibodies against E-cadherin, occluding, and claudin I, and densitometry analysis of Western blots (*n* = 15, from more than 3 independent experiments). *$*P < 0.05$ vs. control.

MBG induced upregulation of vimentin expression with a maximal effect after 72 h of treatment (Fig. 5). MBG also stimulates the expression of fibronectin with a maximal effect at 72–96 h of treatment (Fig. 5). Immunoblotting of proteins extracted from LLC-PK1 cells at all time points showed that MBG induced upregulation of vimentin and fibronectin as early as 24 h of treatment (Fig. 7). We also assessed the effect of MBG on collagen I expression in LLC-PK1 cells. Collagen I secretion was increased twofold in cell culture supernatants treated with MBG (Fig. 8).

MBG governs expression and subcellular localization of the transcription repressor Snail. Several transcription factors govern EMT in tumor and benign epithelial cells including the zinc finger protein Snail (9, 13, 53, 63, 64). In untreated LLC-PK1 cells, the Snail protein was present in the cytoplasm of $39 \pm 6\%$ of the cells, homogeneously in the nuclei of $12\% \pm 6$ of cells, and in $14 \pm 3\%$ of the cells in the nuclear periphery (Fig. 9). At 24 h posttreatment, the total level of Snail expres-

Fig. 8. Effect of 100 nM MBG on expression of collagen I. ELISA for collagen I secretion into growth media. *$P < 0.05$, **$P < 0.001$ vs. control ($n = 9$ from 3 independent experiments).

sion was increased and remained elevated during the experimental time span as demonstrated by Western blotting (Fig. 10*B*). At 24 h posttreatment, Snail was localized in the nuclei of $72 \pm 4\%$ of the cells and in the nuclear periphery in $14 \pm 3\%$ of the cells, and only $4 \pm 2\%$ of the cells displayed cytosolic Snail location. Although at 48 h, the total expression of Snail reached a maximal level, the protein presentation in nuclei was decreased to approximately one-half of that noted at 24 h ($39 \pm 6\%$ homogenous and $20 \pm 4\%$ in periphery) and drastically increased in the cytoplasm ($22 \pm 4\%$). At 72 h of MBG treatment, a second wave of nuclear translocation of Snail protein was observed. At that time, $76 \pm 5\%$ of cells showed homogenous nuclear staining for Snail, and in only $6 \pm 2\%$ of the cells, Snail was present in the nuclear periphery. Redistribution of Snail protein made its next turn after 96 h of MBG treatment. At that time in the majority of cells ($80 \pm 3\%$), Snail was located in the nuclear periphery, only $8 \pm 3\%$ of the cells displayed homogenous nuclear staining, and $10 \pm 2\%$ of the cells showed cytosolic staining for Snail. Western blotting of proteins extracted from whole cells or from nuclear fractions confirmed that MBG not only upregulates expression of Snail protein but it also induces its relocation to nuclei (Fig. 10).

MBG-induced EMT of LLC-PK1 cells and signaling though Na^+-K^+-ATPase. We analyzed whether the MBG effects on the transformation of LLC-PK1 cells are due to inhibition of Na^+-K^+-ATPase (Table 1). At a concentration of 100 nM, MBG, as assessed by $^{86}Rb^+$ uptake, does not inhibit pumping activity of Na^+-K^+-ATPase at 24 h posttreatment. Furthermore, inhibition was not recorded at 48, 72, or 96 h (not shown) of MBG treatment. At the same time, ouabain at a concentration of 50 nM inhibits more than half of the pumping activity. MBG treatment caused a slight but statistically significant decrease in the protein level of the α-subunit of Na^+-K^+-ATPase after 96 h of treatment with MBG (Fig. 11). This observation is an agreement with previous findings that ouabain and to a less extent MBG caused endocytosis of the α-subunit of Na^+-K^+-ATPase in LLC-PK1 cells (42, 43).

DISCUSSION

A number of recent studies (73, 74) revealed that endogenous CTSs control multiple physiological functions of mammalian organisms, e.g., blood pressure, sodium homeostasis, and cardiac activity. Presumably, all CTSs transmit their ex-
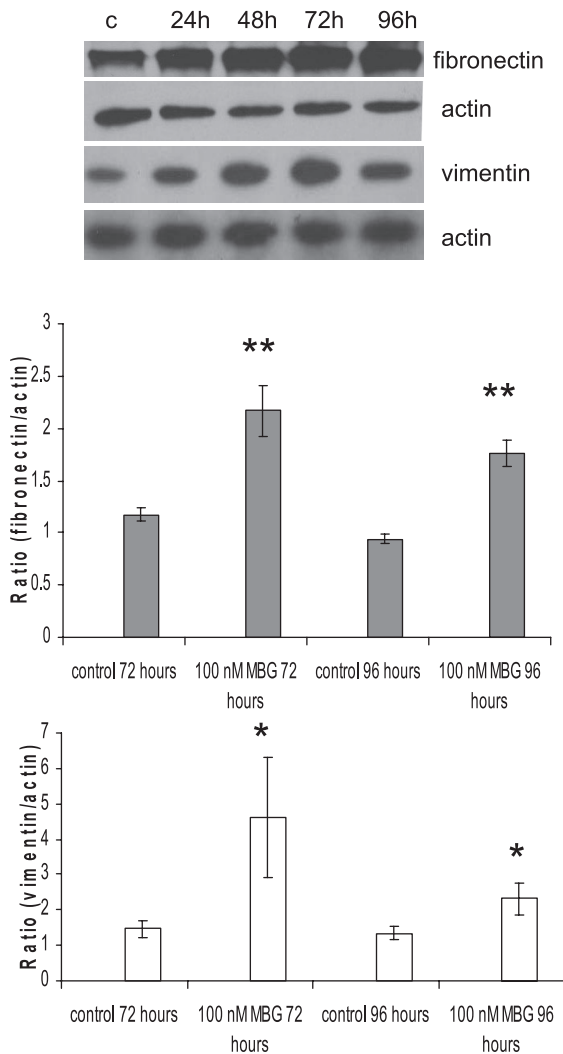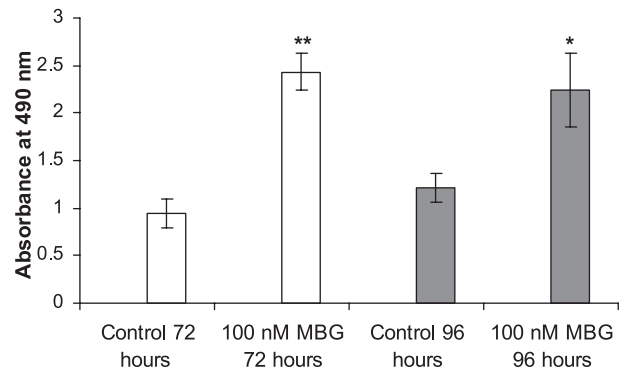

Fig. 7. MBG induced robust stimulation of mesenchymal marker proteins fibronectin and vimentin expression in LLC-PK1 after 96 h of treatment. Representative Western blots for proteins extracted from LLC-PK1 cells at different time points and densitometry analysis of Western blots ($n = 9$, from 3 independent experiments) probed with fibronectin and vimentin antibodies, respectively. *$P < 0.05$, **$P < 0.001$ vs. control.
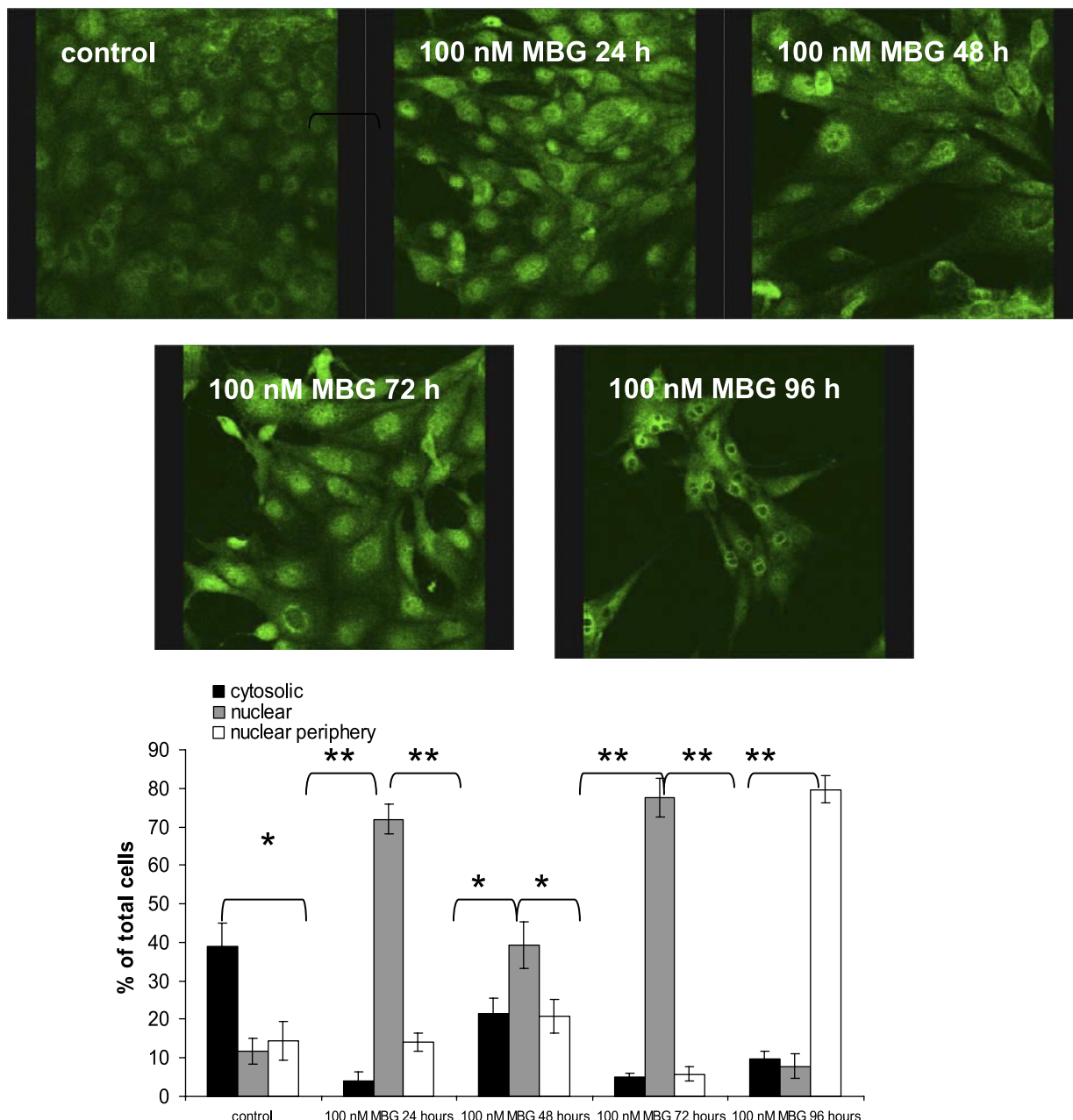
Fig. 9. Immunofluorescence staining of LLC-PK1 cells treated with 100 nM of MBG for different time points demonstrated that MBG induced the expression and relocation of Snail during treatment. Note that the control cells expressed basal level of Snail located mostly in cytoplasm; 24 h of MBG treatment resulted in translocation of Snail into nuclei of ~70% of cells, while at 48 h, <40% percentage of cells demonstrated nuclear staining for Snail. At 72 h, the majority of cells contained Snail in nuclei. Although at 96 h Snail still was residing in the nuclei, its distribution in the nuclei changed from homogeneous to peripheral. The percentage of cells, showing specific accumulation of Snail protein in cellular compartments (cytosolic, nuclear, and nuclear periphery), was estimated by counting the number cells demonstrating a clear specific localization of Snail relative to the total number of cells present on at least 8 randomly chosen fields. *$P < 0.05$ vs. control, **$P < 0.001$ vs. control.

tracellular signal through the same molecule, the α-subunit of Na$^+$-K$^+$-ATPase (16, 21). MBG and ouabain belong to two different subclasses of CTSs: bufadienolides, containing a five-membered lactone ring, and cardienolides with six-membered lactone, respectively. The structure of lactone ring moiety of CTS has been shown to determine binding and inhibitory activities of CTSs (21).

We have shown that administration of MBG to rats induced kidney fibrosis. MBG likely promoted fibrosis by targeting different populations of renal cells. First, direct activation of

interstitial fibroblasts could be accounted for roughly a twofold increase in collagen I content in the tubular interstitium. This level of collagen I increment by MBG, ouabain, and digoxin has recently been shown in several types of fibroblasts (19, 20). Second, MBG, presumably indirectly, through stimulation of the renin-angiotensin-aldosterone system induced TGF-β$_1$ secretion and consequent activation of perivascular mesenchymal cells and fibrotic scar formation. Recent investigations demonstrate that pericytes and bone marrow cells (41), as well as fibroblasts, emerged through EMT (89) contribute to the de-
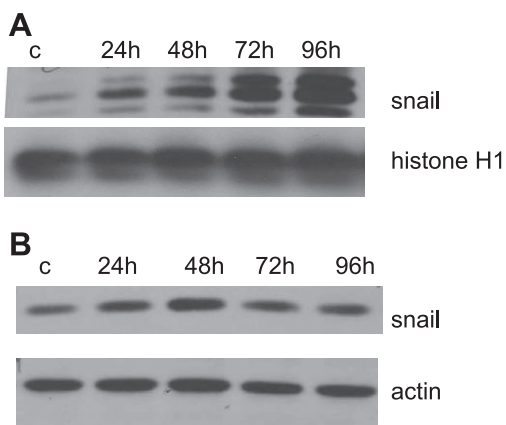
Fig. 10. MBG upregulated and governed nuclear translocation of the transcription factor Snail. Western blots of whole cellular (*A*) and nuclear (*B*) extracts probed against anti-Snail antibody.

velopment of the perivascular fibrosis in the kidney. Whether MBG alone could have any effect on these types of cells in triggering renal fibrosis needs to be studied. Third, de novo expression of the transcription factor Snail could initiate EMT in renal tubules thus promoting tubular degeneration and fibrotic scar formation.

The transcription factor Snail is an evolutionary conserved protein: its homologs have been associated with EMT across the animal kingdom (50). Activation of Snail in the adult kidney has been sufficient to induce fibrosis (8). In addition, the attenuation of renal fibrosis by the synthetic vitamin D paricalcitol and the chemokine receptor agonist BX471 has been correlated with downregulation of transcription factor Snail (36, 77). Renal fibrosis and upregulation of Snail in kidneys of the MBG-administered rats could be due to the activation of the renin-angiotensin-aldosterone system and consequent upregulation of the profibrotic TGF-β and its receptor system (10).

We have provided evidence that MBG alone can trigger EMT in renal epithelia. In particular, treatment of LLC-PK1 cells with 100 nM MBG upregulates the expression of the mesenchymal protein markers vimentin, fibronectin, and collagen I and induces cell scattering and invasive motility. A particular peculiarity of MBG-induced EMT was the finding that this steroid induces transformation of epithelial cells to the mesenchyme without significant downregulation of epithelial proteins. In a majority of the described EMT models, dramatic downregulation of E-cadherin and detachment of cells precede EMT (11, 30, 39, 53, 57, 78, 90, 92). When LLC-PK1 cells were treated with ouabain at concentration 10–100 nM, we did find the decrease in E-cadherin protein expression and cell detachment, but ouabain was unable to trigger mesenchymal gene programming. Cell detachment and β-catenin translocation to the nucleus in the presence of 1 μM of ouabain were shown recently in MDCK cells. The authors did not report whether MDCK cells in these experiments underwent EMT (12, 37). Another study showed that a concentration of 1 μM ouabain was toxic for MDCK cells (1).

EMT in LLC-PK1 cells seen in the presence of MBG is accompanied by upregulation of Snail protein. In a majority of described embryonic, carcinoma, and adult EMT, the expression of Snail protein is associated with *1*) acquisition by

epithelial cells a fibroblastoid, invasive phenotype; *2*) downregulation of epithelial proteins, especially E-cadherin; and *3*) upregulation of mesenchymal proteins. The set of all these changes is known as complete EMT (53, 63, 64). Nevertheless, in some developmental processes or during wound healing, migrating cells expressing high levels of Snail show only transient loss of polarity by redistribution of tight- or adherent-junction proteins (so called partial EMT; Refs. 27, 32). Because the MBG-treated LLC-PK1 cells had only mild downregulation of their tight/adherent junction proteins, we would rather classify this process as a partial EMT. In most epithelial cells, Snail is not detected in the absence of stimuli (9). Yet, there are reports in which E-cadherin and Snail are both detected in the same cell lines. In these cells, Snail function is controlled by its intracellular location through phosphorylation by cytosolic and nuclear protein kinase GSKβ3 (87, 94). Phosphorylated Snail protein is much less active as a repressor of E-cadherin and an inducer of the mesenchymal genes (15). We suggest that the partial EMT seen in LLC-PK1 could be a consequence of high basal levels of Snail protein. Since MBG treatment induced translocation of the transcription repressor Snail to the nuclei at 24 and 72 h, we presume that MBG could regulate Snail phosphorylation as well. After 96 h of MBG treatment, Snail localized in the periphery of the nuclei, suggesting its association with the inner nuclear membrane. Sequestering of transcription factors on the inner nuclear membrane restricts their access to target genes and temporarily limits their transactivation/transrepression abilities (31).

Currently, we cannot exclude that other transcription regulators, besides Snail, could be involved in activation of mesenchymal genes in the response to MBG treatment. However, our preliminary studies revealed that quenching reactive oxygen species, which was shown to upregulate the expression of Snail protein (70), completely inhibited MBG-induced EMT of LLC-PK1 cells. Since MBG treatment did not significantly decrease the amount of E-cadherin in LLC-PK1 cells, we, as expected, did not find any alterations in total β-catenin expression levels and its subcellular localization. Nevertheless, transcription factor TCF4/LEF-1, a master-gene of EMT, was de novo expressed in LLC-PK1 cells after 72–96 h of treatment

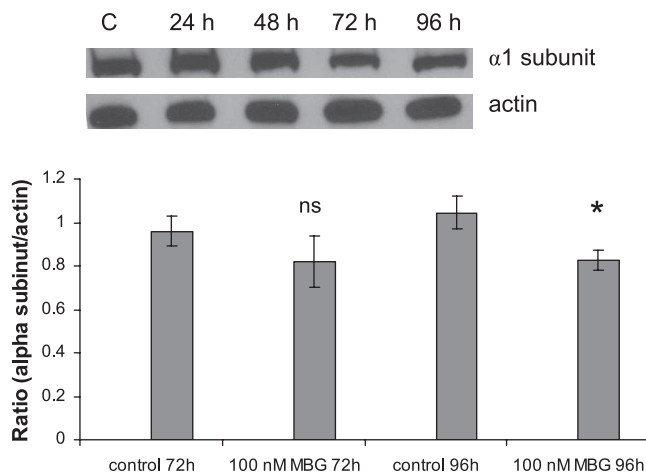Fig. 11. Protein level of the α_1-subunit of Na$^+$-K$^+$-ATPase was moderately but significantly decreased after treatment with MBG for 96 h, as shown by representative Western blot and densitometry analysis ($n = 10$). $P < 0.05$ vs. control.

with 100 nM MBG (not shown). In the absence of transcriptional coactivator β-catenin, TCF4/LEF-1 is characterized by a weak binding affinity to promotor regions (2). Since we did not detect β-catenin in nuclei, the transcriptional effectiveness of TCF4/LEF-1 in MBG-treated LLC-PK1 cells remains unclear.

Unlike most epithelial cells, LLC-PK1 cells are resistant to TGF-β_1-induced EMT in intact confluent monolayers. These cells are susceptible to EMT induced by TGF-β_1 only if cell-cell contacts are prevented by various experimental conditions including low cell density (51). In this contact-dependent model of EMT in LLC-PK1 cells, TGF-β_1 has triggered dramatic downregulation of E-cadherin after 72 h of treatment. In our initial experiments, when confluent and subconfluent cultures of LLC-PK1 cells were treated with TGF-β_1, these effects were confirmed. Moreover, when subconfluent (50–60% of cell density) cultures of LLC-PK1 cells were treated with MBG in concentrations from 0.1 to 100 nM for 96 h, we documented a concentration-dependent downregulation of E-cadherin protein levels. Yet, in these experiments, we did not find any fibroblast-like alteration of LLC-PK1 cells. This was a surprising observation, since Na^+-K^+-ATPase resides in the basolateral aspect of the established epithelial monolayer and it was reasonable to suggest that in subconfluent cultures Na^+-K^+-ATPase would be more accessible for the MBG ligand (58–60). We propose that a pool of Na^+-K^+-ATPase molecules, which specifically resides in the apical junctional complex in the polarized epithelia and connected through accessory proteins to the cytoskeleton, may play a crucial role in the MBG effect on transdifferentiation of LLC-PK1 cells (59).

The plasma concentration of MBG after 4 wk of administration to rats reached nearly 0.5 nM, while EMT in LLC-PK1 cells occurred at much higher concentrations (50–100 nM). These discrepancies may be attributed to the different sensitivities of MBG to the rodent and porcine α_1-subunit of Na^+-K^+-ATPase (22, 43). Concentrations of MBG used in our in vitro experiments were below levels at which changes of the pumping activity of Na^+-K^+-ATPase could be recorded by $^{86}Rb^+$ uptake. On the other hand, ouabain concentrations of 50–100 nM inhibited Na^+-K^+-ATPase activity in the same cells substantially over time and eventually caused cell death. Therefore, the absence of significant EMT under these conditions for ouabain was not surprising. We have previously demonstrated that although equimolar amounts of ouabain and MBG have similar acute (30 min) effects on $^{86}Rb^+$ uptake, equimolar amounts of MBG induces much smaller amounts of Na^+-K^+-ATPase endocytosis in LLC-PK1 cells than ouabain, and, over longer periods of time, MBG inhibits $^{86}Rb^+$ uptake much less than ouabain (43). We would therefore speculate that long-term exposure to substantial amounts (e.g., 100 nM) of ouabain induces programmed cell death whereas smaller amounts of ouabain promote cell growth and proliferation (14, 84), processes shown to be incompatible with EMT (54). We also speculate that MBG, in addition to activation of proteins within the Na^+-K^+-ATPase signalosome complex, might also induce cell cycle arrest, a necessary prerequisite of the dedifferentiation programs such as EMT (54, 79, 82). Notably, a similar difference between patterns of ouabain- and MBG-induced signaling have been previously reported in another renal epithelial cell line, MDCK, in which ouabain not MBG induced cell death (1).

In summary, we report for the first time that CTS, in the form of MBG, has the capacity in vivo and in vitro to induce the EMT process, which is directly involved in the development of organ fibrosis. Our findings further support the innovatory discovery of the nonpumping, signaling function of Na^+-K^+-ATPase; furthermore, they broaden our understanding of endogenous CTS actions and provide important information for the prevention and treatment of fibrotic diseases.

REFERENCES

1. **Akimova OA, Bagrov AY, Lopina OD, Kamernitsky AV, Tremblay J, Hamet P, Orlov SN.** Cardiotonic steroids differentially affect intracellular Na+ and [Na+]i/[K+]i-independent signaling in C7-MDCK cells. *J Biol Chem* 280: 832–839, 2005.
2. **Arce L, Yokoyama NN, Waterman ML.** Diversity of LEF/TCF action in development and disease. *Oncogene* 25: 7492–7504, 2006.
3. **Averina IV, Tapilskaya NI, Reznik VA, Frolova EV, Fedorova OV, Lakatta EG, Bagrov AY.** Endogenous Na/K-ATPase inhibitors in patients with preeclampsia. *Cell Mol Biol (Noisy-le-grand)* 52: 19–23, 2006.
4. **Bagrov AY, Fedorova OV.** Cardenolide and bufadienolide ligands of the sodium pump. How they work together in NaCl sensitive hypertension. *Front Biosci* 10: 2250–2256, 2005.
5. **Bagrov AY, Fedorova OV, Dmitrieva RI, French AW, Anderson DE.** Plasma marinobufagenin-like and ouabain-like immunoreactivity during saline volume expansion in anesthetized dogs. *Cardiovasc Res* 31: 296–305, 1996.
6. **Bagrov AY, Roukoyatkina NI, Pinaev AG, Dmitrieva RI, Fedorova OV.** Effects of two endogenous Na+,K(+)-ATPase inhibitors, marinobufagenin and ouabain, on isolated rat aorta. *Eur J Pharmacol* 274: 151–158, 1995.
7. **Bagrov YY, Manusova NB, Egorova IA, Fedorova OV, Bagrov AY.** Endogenous digitalis-like ligands and Na/K-ATPase inhibition in experimental diabetes mellitus. *Front Biosci* 10: 2257–2262, 2005.
8. **Boutet A, De Frutos CA, Maxwell PH, Mayol MJ, Romero J, Nieto MA.** Snail activation disrupts tissue homeostasis and induces fibrosis in the adult kidney. *EMBO J* 25: 5603–5613, 2006.
9. **Boutet A, Esteban MA, Maxwell PH, Nieto MA.** Reactivation of Snail genes in renal fibrosis and carcinomas: a process of reversed embryogenesis? *Cell Cycle* 6: 638–642, 2007.
10. **Carvajal G, Rodriguez-Vita J, Rodrigues-Diez R, Sanchez-Lopez E, Ruperez M, Cartier C, Esteban V, Ortiz A, Egido J, Mezzano SA, Ruiz-Ortega M.** Angiotensin II activates the Smad pathway during epithelial mesenchymal transdifferentiation. *Kidney Int* 74: 551–553, 2008.
11. **Christofori G.** New signals from the invasive front. *Nature* 441: 444–450, 2006.
12. **Contreras RG, Flores-Maldonado C, Lazaro A, Shoshani L, Flores-Benitez D, Larre I, Cereijido M.** Ouabain binding to Na+,K+-ATPase relaxes cell attachment and sends a specific signal (NACos) to the nucleus. *J Membr Biol* 198: 147–158, 2004.
13. **De Craene B, van Roy F, Berx G.** Unraveling signalling cascades for the Snail family of transcription factors. *Cell Signal* 17: 535–547, 2005.
14. **Dmitrieva RI, Doris PA.** Ouabain is a potent promoter of growth and activator of ERK1/2 in ouabain-resistant rat renal epithelial cells. *J Biol Chem* 278: 28160–28166, 2003.
15. **Dominguez D, Montserrat-Sentis B, Virgos-Soler A, Guaita S, Grueso J, Porta M, Puig I, Baulida J, Franci C, Garcia de Herreros A.**

Phosphorylation regulates the subcellular location and activity of the snail transcriptional repressor. *Mol Cell Biol* 23: 5078–5089, 2003.

16. **Dostanic-Larson I, Lorenz JN, Van Huysse JW, Neumann JC, Moseley AE, Lingrel JB.** Physiological role of the α_1- and α_2-isoforms of the Na^+-K^+-ATPase and biological significance of their cardiac glycoside binding site. *Am J Physiol Regul Integr Comp Physiol* 290: R524–R528, 2006.

17. **Eddy AA.** Molecular basis of renal fibrosis. *Pediatr Nephrol* 15: 290–301, 2000.

18. **Eddy AA, Neilson EG.** Chronic kidney disease progression. *J Am Soc Nephrol* 17: 2964–2966, 2006.

19. **El-Okdi N, Smaili S, Raju V, Shidyak A, Gupta S, Fedorova L, Elkareh J, Periyasamy SM, Shapiro AP, Kahaleh MB, Malhotra D, Xie Z, Chin KV, Shapiro JI.** The effects of cardiotonic steroids on dermal collagen synthesis and wound healing. *J Appl Physiol* 105: 30–36, 2008.

20. **Elkareh J, Kennedy DJ, Yashaswi B, Vetteth S, Shidyak A, Kim EG, Smaili S, Periyasamy SM, Hariri IM, Fedorova L, Liu J, Wu L, Kahaleh MB, Xie Z, Malhotra D, Fedorova OV, Kashkin VA, Bagrov AY, Shapiro JI.** Marinobufagenin stimulates fibroblast collagen production and causes fibrosis in experimental uremic cardiomyopathy. *Hypertension* 49: 215–224, 2007.

21. **Farr CD, Burd C, Tabet MR, Wang X, Welsh WJ, Ball WJ Jr.** Three-dimensional quantitative structure-activity relationship study of the inhibition of $Na(+),K(+)$-ATPase by cardiotonic steroids using comparative molecular field analysis. *Biochemistry* 41: 1137–1148, 2002.

22. **Fedorova OV, Agalakova NI, Morrell CH, Lakatta EG, Bagrov AY.** ANP differentially modulates marinobufagenin-induced sodium pump inhibition in kidney and aorta. *Hypertension* 48: 1160–1168, 2006.

23. **Fedorova OV, Anderson DE, Bagrov AY.** Plasma marinobufagenin-like and ouabain-like immunoreactivity in adrenocorticotropin-treated rats. *Am J Hypertens* 11: 796–802, 1998.

24. **Fedorova OV, Talan MI, Agalakova NI, Lakatta EG, Bagrov AY.** Endogenous ligand of alpha(1) sodium pump, marinobufagenin, is a novel mediator of sodium chloride–dependent hypertension. *Circulation* 105: 1122–1127, 2002.

25. **Garraffo HM, Gros EG.** Biosynthesis of bufadienolides in toads. VI. Experiments with [1,2–3H]cholesterol, [21–14C]coprostanol, and 5 beta-[21–14 C]pregnanolone in the toad Bufo arenarum. *Steroids* 48: 251–257, 1986.

26. **Gheorghiade M, van Veldhuisen DJ, Colucci WS.** Contemporary use of digoxin in the management of cardiovascular disorders. *Circulation* 113: 2556–2564, 2006.

27. **Grunert S, Jechlinger M, Beug H.** Diverse cellular and molecular mechanisms contribute to epithelial plasticity and metastasis. *Nat Rev Mol Cell Biol* 4: 657–665, 2003.

28. **Haas M, Wang H, Tian J, Xie Z.** Src-mediated inter-receptor cross-talk between the Na+/K+-ATPase and the epidermal growth factor receptor relays the signal from ouabain to mitogen-activated protein kinases. *J Biol Chem* 277: 18694–18702, 2002.

29. **Hamlyn JM, Lu ZR, Manunta P, Ludens JH, Kimura K, Shah JR, Laredo J, Hamilton JP, Hamilton MJ, Hamilton BP.** Observations on the nature, biosynthesis, secretion and significance of endogenous ouabain. *Clin Exp Hypertens* 20: 523–533, 1998.

30. **Hay ED.** The mesenchymal cell, its role in the embryo, and the remarkable signaling mechanisms that create it. *Dev Dyn* 233: 706–720, 2005.

31. **Heessen S, Fornerod M.** The inner nuclear envelope as a transcription factor resting place. *EMBO Rep* 8: 914–919, 2007.

32. **Huber MA, Kraut N, Beug H.** Molecular requirements for epithelial-mesenchymal transition during tumor progression. *Curr Opin Cell Biol* 17: 548–558, 2005.

33. **Kennedy DJ, Vetteth S, Periyasamy SM, Kanj M, Fedorova L, Khouri S, Kahaleh MB, Xie Z, Malhotra D, Kolodkin NI, Lakatta EG, Fedorova OV, Bagrov AY, Shapiro JI.** Central role for the cardiotonic steroid marinobufagenin in the pathogenesis of experimental uremic cardiomyopathy. *Hypertension* 47: 488–495, 2006.

34. **Komiyama Y, Dong XH, Nishimura N, Masaki H, Yoshika M, Masuda M, Takahashi H.** A novel endogenous digitalis, telocinobufagin, exhibits elevated plasma levels in patients with terminal renal failure. *Clin Biochem* 38: 36–45, 2005.

35. **Kotova O, Al-Khalili L, Talia S, Hooke C, Fedorova OV, Bagrov AY, Chibalin AV.** Cardiotonic steroids stimulate glycogen synthesis in human skeletal muscle cells via a Src- and ERK1/2-dependent mechanism. *J Biol Chem* 281: 20085–20094, 2006.

36. **Lange-Sperandio B, Trautmann A, Eickelberg O, Jayachandran A, Oberle S, Schmidutz F, Rodenbeck B, Homme M, Horuk R, Schaefer F.** Leukocytes induce epithelial to mesenchymal transition after unilateral ureteral obstruction in neonatal mice. *Am J Pathol* 171: 861–871, 2007.

37. **Larre I, Ponce A, Fiorentino R, Shoshani L, Contreras RG, Cereijido M.** Contacts and cooperation between cells depend on the hormone ouabain. *Proc Natl Acad Sci USA* 103: 10911–10916, 2006.

38. **Laurière M.** A semidry electroblotting system efficiently transfers both high- and low-molecular-weight proteins separated by SDS-PAGE. *Anal Biochem* 212: 206–211, 1993.

39. **Lee JM, Dedhar S, Kalluri R, Thompson EW.** The epithelial-mesenchymal transition: new insights in signaling, development, and disease. *J Cell Biol* 172: 973–981, 2006.

40. **Li JH, Wang W, Huang XR, Oldfield M, Schmidt AM, Cooper ME, Lan HY.** Advanced glycation end products induce tubular epithelial-myofibroblast transition through the RAGE-ERK1/2 MAP kinase signaling pathway. *Am J Pathol* 164: 1389–1397, 2004.

41. **Lin SL, Kisseleva T, Brenner DA, Duffield JS.** Pericytes and perivascular fibroblasts are the primary source of collagen-producing cells in obstructive fibrosis of the kidney. *Am J Pathol* 173: 1617–1627, 2008.

42. **Liu J, Kesiry R, Periyasamy SM, Malhotra D, Xie Z, Shapiro JI.** Ouabain induces endocytosis of plasmalemmal Na/K-ATPase in LLC-PK1 cells by a clathrin-dependent mechanism. *Kidney Int* 66: 227–241, 2004.

43. **Liu J, Periyasamy SM, Gunning W, Fedorova OV, Bagrov AY, Malhotra D, Xie Z, Shapiro JI.** Effects of cardiac glycosides on sodium pump expression and function in LLC-PK1 and MDCK cells. *Kidney Int* 62: 2118–2125, 2002.

44. **Liu L, Zhao X, Pierre SV, Askari A.** Association of PI3K-Akt signaling pathway with digitalis-induced hypertrophy of cardiac myocytes. *Am J Physiol Cell Physiol* 293: C1489–C1497, 2007.

45. **Lopatin DA, Ailamazian EK, Dmitrieva RI, Shpen VM, Fedorova OV, Doris PA, Bagrov AY.** Circulating bufodienolide and cardenolide sodium pump inhibitors in preeclampsia. *J Hypertens* 17: 1179–1187, 1999.

46. **Lozano E, Cano A.** Cadherin/catenin complexes in murine epidermal keratinocytes: E-cadherin complexes containing either beta-catenin or plakoglobin contribute to stable cell-cell contacts. *Cell Adhes Commun* 6: 51–67, 1998.

47. **Manotham K, Tanaka T, Matsumoto M, Ohse T, Inagi R, Miyata T, Kurokawa K, Fujita T, Ingelfinger JR, Nangaku M.** Transdifferentiation of cultured tubular cells induced by hypoxia. *Kidney Int* 65: 871–880, 2004.

48. **Manunta P, Hamilton BP, Hamlyn JM.** Salt intake and depletion increase circulating levels of endogenous ouabain in normal men. *Am J Physiol Regul Integr Comp Physiol* 290: R553–R559, 2006.

49. **Manunta P, Iacoviello M, Forleo C, Messaggio E, Hamlyn JM, Lucarelli K, Guida P, Romito R, De Tommasi E, Bianchi G, Rizzon P, Pitzalis MV.** High circulating levels of endogenous ouabain in the offspring of hypertensive and normotensive individuals. *J Hypertens* 23: 1677–1681, 2005.

50. **Manzanares M, Locascio A, Nieto MA.** The increasing complexity of the Snail gene superfamily in metazoan evolution. *Trends Genet* 17: 178–181, 2001.

51. **Masszi A, Fan L, Rosivall L, McCulloch CA, Rotstein OD, Mucsi I, Kapus A.** Integrity of cell-cell contacts is a critical regulator of TGF-beta 1-induced epithelial-to-myofibroblast transition: role for beta-catenin. *Am J Pathol* 165: 1955–1967, 2004.

52. **McMorrow T, Gaffney MM, Slattery C, Campbell E, Ryan MP.** Cyclosporine A induced epithelial-mesenchymal transition in human renal proximal tubular epithelial cells. *Nephrol Dial Transplant* 20: 2215–2225, 2005.

53. **Medici D, Hay ED, Goodenough DA.** Cooperation between snail and LEF-1 transcription factors is essential for TGF-beta1-induced epithelial-mesenchymal transition. *Mol Biol Cell* 17: 1871–1879, 2006.

54. **Mejlvang J, Kriajevska M, Vandewalle C, Chernova T, Sayan AE, Berx G, Mellon JK, Tulchinsky E.** Direct repression of cyclin D1 by SIP1 attenuates cell cycle progression in cells undergoing an epithelial mesenchymal transition. *Mol Biol Cell* 18: 4615–4624, 2007.

55. **Miyakawa-Naito A, Uhlen P, Lal M, Aizman O, Mikoshiba K, Brismar H, Zelenin S, Aperia A.** Cell signaling microdomain with Na,K-ATPase and inositol 1,4,5-trisphosphate receptor generates calcium oscillations. *J Biol Chem* 278: 50355–50361, 2003.

56. **Mohammadi K, Kometiani P, Xie Z, Askari A.** Role of protein kinase C in the signal pathways that link Na+/K+-ATPase to ERK1/2. *J Biol Chem* 276: 42050–42056, 2001.

57. **Nawshad A, Lagamba D, Polad A, Hay ED.** Transforming growth factor-beta signaling during epithelial-mesenchymal transformation: implications for embryogenesis and tumor metastasis. *Cells Tissues Organs* 179: 11–23, 2005.

58. **Nelson WJ.** Adaptation of core mechanisms to generate cell polarity. *Nature* 422: 766–774, 2003.

59. **Nelson WJ.** Epithelial cell polarity from the outside looking in. *News Physiol Sci* 18: 143–146, 2003.

60. **Nelson WJ, Veshnock PJ.** Ankyrin binding to (Na++ K+)ATPase and implications for the organization of membrane domains in polarized cells. *Nature* 328: 533–536, 1987.

61. **Nightingale J, Patel S, Suzuki N, Buxton R, Takagi KI, Suzuki J, Sumi Y, Imaizumi A, Mason RM, Zhang Z.** Oncostatin M, a cytokine released by activated mononuclear cells, induces epithelial cell-myofibroblast transdifferentiation via Jak/Stat pathway activation. *J Am Soc Nephrol* 15: 21–32, 2004.

62. **Okada H, Kalluri R.** Cellular and molecular pathways that lead to progression and regression of renal fibrogenesis. *Curr Mol Med* 5: 467–474, 2005.

63. **Peinado H, Olmeda D, Cano A.** Snail, Zeb and bHLH factors in tumour progression: an alliance against the epithelial phenotype? *Nat Rev Cancer* 7: 415–428, 2007.

64. **Peinado H, Quintanilla M, Cano A.** Transforming growth factor beta-1 induces snail transcription factor in epithelial cell lines: mechanisms for epithelial mesenchymal transitions. *J Biol Chem* 278: 21113–21123, 2003.

65. **Pervaiz MH, Dickinson MG, Yamani M.** Is digoxin a drug of the past? *Cleve Clin J Med* 73: 821–824, 826, 829–832 passim, 2006.

66. **Pitzalis MV, Hamlyn JM, Messaggio E, Iacoviello M, Forleo C, Romito R, de Tommasi E, Rizzon P, Bianchi G, Manunta P.** Independent and incremental prognostic value of endogenous ouabain in idiopathic dilated cardiomyopathy. *Eur J Heart Fail* 8: 179–186, 2006.

67. **Pollack V, Sarkozi R, Banki Z, Feifel E, Wehn S, Gstraunthaler G, Stoiber H, Mayer G, Montesano R, Strutz F, Schramek H.** Oncostatin M-induced effects on EMT in human proximal tubular cells: differential role of ERK signaling. *Am J Physiol Renal Physiol* 293: F1714–F1726, 2007.

68. **Puschett JB.** Vascular effects of the bufodienolides. *Trans Am Clin Climatol Assoc* 119: 103–112, 2008.

69. **Radisky DC, Kenny PA, Bissell MJ.** Fibrosis and cancer: do myofibroblasts come also from epithelial cells via EMT? *J Cell Biochem* 101: 830–839, 2007.

70. **Radisky DC, Levy DD, Littlepage LE, Liu H, Nelson CM, Fata JE, Leake D, Godden EL, Albertson DG, Nieto MA, Werb Z, Bissell MJ.** Rac1b and reactive oxygen species mediate MMP-3-induced EMT and genomic instability. *Nature* 436: 123–127, 2005.

71. **Rhyu DY, Yang Y, Ha H, Lee GT, Song JS, Uh ST, Lee HB.** Role of reactive oxygen species in TGF-beta1-induced mitogen-activated protein kinase activation and epithelial-mesenchymal transition in renal tubular epithelial cells. *J Am Soc Nephrol* 16: 667–675, 2005.

72. **Sato M, Muragaki Y, Saika S, Roberts AB, Ooshima A.** Targeted disruption of TGF-beta1/Smad3 signaling protects against renal tubulointerstitial fibrosis induced by unilateral ureteral obstruction. *J Clin Invest* 112: 1486–1494, 2003.

73. **Schoner W, Scheiner-Bobis G.** Endogenous and exogenous cardiac glycosides and their mechanisms of action. *Am J Cardiovasc Drugs* 7: 173–189, 2007.

74. **Schoner W, Scheiner-Bobis G.** Endogenous and exogenous cardiac glycosides: their roles in hypertension, salt metabolism, and cell growth. *Am J Physiol Cell Physiol* 293: C509–C536, 2007.

75. **Shimada K, Nambara T.** Isolation and characterization of cardiotonic steroid conjugates from the skin of Bufo marinus (L.) Schneider. *Chem Pharm Bull (Tokyo)* 27: 1881–1886, 1979.

76. **Strutz F, Zeisberg M, Ziyadeh FN, Yang CQ, Kalluri R, Muller GA, Neilson EG.** Role of basic fibroblast growth factor-2 in epithelial-mesenchymal transformation. *Kidney Int* 61: 1714–1728, 2002.

77. **Tan X, Wen X, Liu Y.** Paricalcitol inhibits renal inflammation by promoting vitamin d receptor-mediated sequestration of NF-κB signaling. *J Am Soc Nephrol* 19: 1741–1752, 2008.

78. **Thiery JP, Sleeman JP.** Complex networks orchestrate epithelial-mesenchymal transitions. *Nat Rev Mol Cell Biol* 7: 131–142, 2006.

79. **Turner FE, Broad S, Khanim FL, Jeanes A, Talma S, Hughes S, Tselepis C, Hotchin NA.** Slug regulates integrin expression and cell proliferation in human epidermal keratinocytes. *J Biol Chem* 281: 21321–21331, 2006.

80. **Uddin MN, Horvat D, Glaser SS, Danchuk S, Mitchell BM, Sullivan DE, Morris CA, Puschett JB.** Marinobufagenin inhibits proliferation and migration of cytotrophoblast and CHO cells. *Placenta* 29: 266–273, 2008.

81. **Uddin MN, Horvat D, Glaser SS, Mitchell BM, Puschett JB.** Examination of the cellular mechanisms by which marinobufagenin inhibits cytotrophoblast function. *J Biol Chem* 283: 17946–17953, 2008.

82. **Vega S, Morales AV, Ocana OH, Valdes F, Fabregat I, Nieto MA.** Snail blocks the cell cycle and confers resistance to cell death. *Genes Dev* 18: 1131–1143, 2004.

83. **Vu HV, Ianosi-Irimie MR, Pridjian CA, Whitbred JM, Durst JM, Bagrov AY, Fedorova OV, Pridjian G, Puschett JB.** Involvement of marinobufagenin in a rat model of human preeclampsia. *Am J Nephrol* 25: 520–528, 2005.

84. **Xie Z.** Molecular mechanisms of Na/K-ATPase-mediated signal transduction. *Ann NY Acad Sci* 986: 497–503, 2003.

85. **Xie Z, Kometiani P, Liu J, Li J, Shapiro JI, Askari A.** Intracellular reactive oxygen species mediate the linkage of Na+/K+-ATPase to hypertrophy and its marker genes in cardiac myocytes. *J Biol Chem* 274: 19323–19328, 1999.

86. **Yang J, Liu Y.** Dissection of key events in tubular epithelial to myofibroblast transition and its implications in renal interstitial fibrosis. *Am J Pathol* 159: 1465–1475, 2001.

87. **Yook JI, Li XY, Ota I, Hu C, Kim HS, Kim NH, Cha SY, Ryu JK, Choi YJ, Kim J, Fearon ER, Weiss SJ.** A Wnt-Axin2-GSK3beta cascade regulates Snail1 activity in breast cancer cells. *Nat Cell Biol* 8: 1398–1406, 2006.

88. **Yuan Z, Cai T, Tian J, Ivanov AV, Giovannucci DR, Xie Z.** Na/K-ATPase tethers phospholipase C and IP3 receptor into a calcium-regulatory complex. *Mol Biol Cell* 16: 4034–4045, 2005.

89. **Zeisberg EM, Potenta SE, Sugimoto H, Zeisberg M, Kalluri R.** Fibroblasts in kidney fibrosis emerge via endothelial-to-mesenchymal transition. *J Am Soc Nephrol* 19: 2282–2287, 2008.

90. **Zeisberg EM, Tarnavski O, Zeisberg M, Dorfman AL, McMullen JR, Gustafsson E, Chandraker A, Yuan X, Pu WT, Roberts AB, Neilson EG, Sayegh MH, Izumo S, Kalluri R.** Endothelial-to-mesenchymal transition contributes to cardiac fibrosis. *Nat Med* 13: 952–961, 2007.

91. **Zeisberg M, Kalluri R.** Fibroblasts emerge via epithelial-mesenchymal transition in chronic kidney fibrosis. *Front Biosci* 13: 6991–6998, 2008.

92. **Zeisberg M, Yang C, Martino M, Duncan MB, Rieder F, Tanjore H, Kalluri R.** Fibroblasts derive from hepatocytes in liver fibrosis via epithelial to mesenchymal transition. *J Biol Chem* 282: 23337–23347, 2007.

93. **Zhang A, Jia Z, Guo X, Yang T.** Aldosterone induces epithelial-mesenchymal transition via ROS of mitochondrial origin. *Am J Physiol Renal Physiol* 293: F723–F731, 2007.

94. **Zhou BP, Deng J, Xia W, Xu J, Li YM, Gunduz M, Hung MC.** Dual regulation of Snail by GSK-3beta-mediated phosphorylation in control of epithelial-mesenchymal transition. *Nat Cell Biol* 6: 931–940, 2004.